



Supplement of

A numerical model for duricrust formation by laterisation

Caroline Fenske et al.

Correspondence to: Caroline Fenske (fenske@ig.cas.cz)

The copyright of individual parts of the supplement might differ from the article licence.

S1 Supplementary Material

S1.1 Varying τ in percolation mode

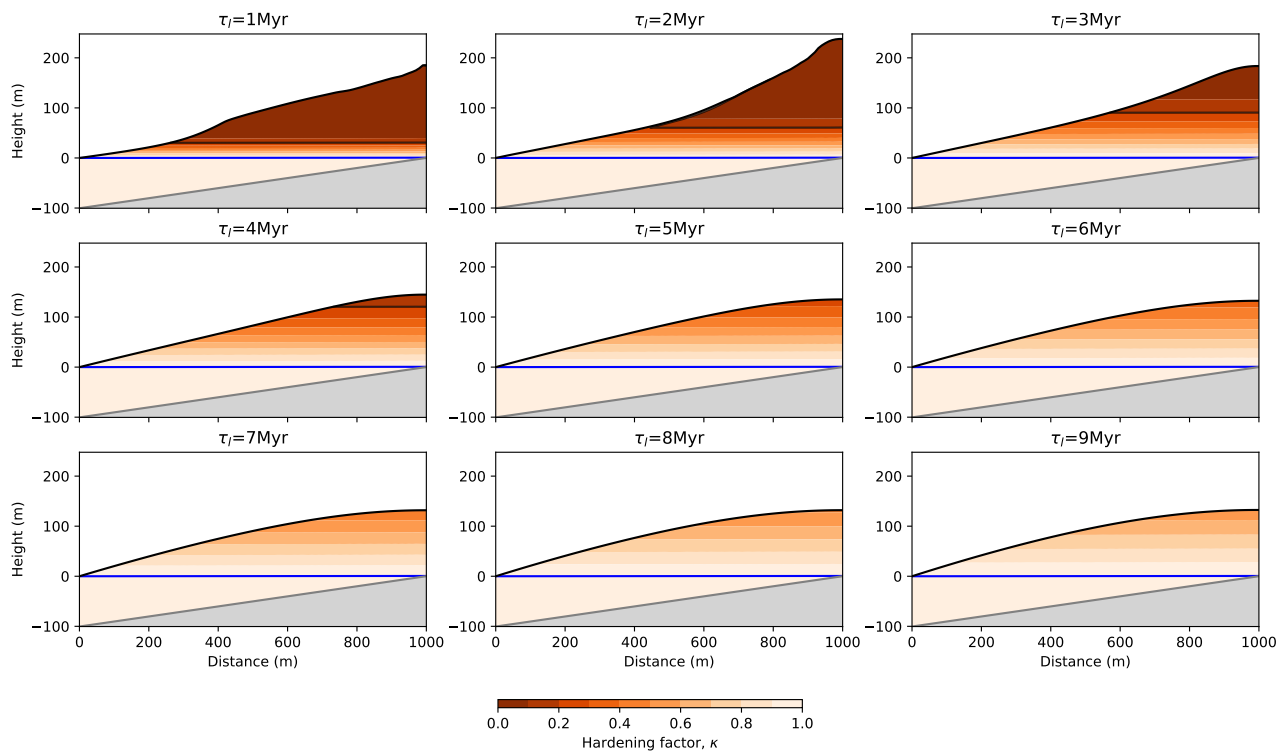


Figure S1. Model behavior with varying τ , the laterisation time scale, in the percolation mode ($C = -1$). Each panel corresponds to the model solution after 20 Myr of evolution with a different value of τ increasing from top left to bottom right.

S1.2 Varying U in percolation mode

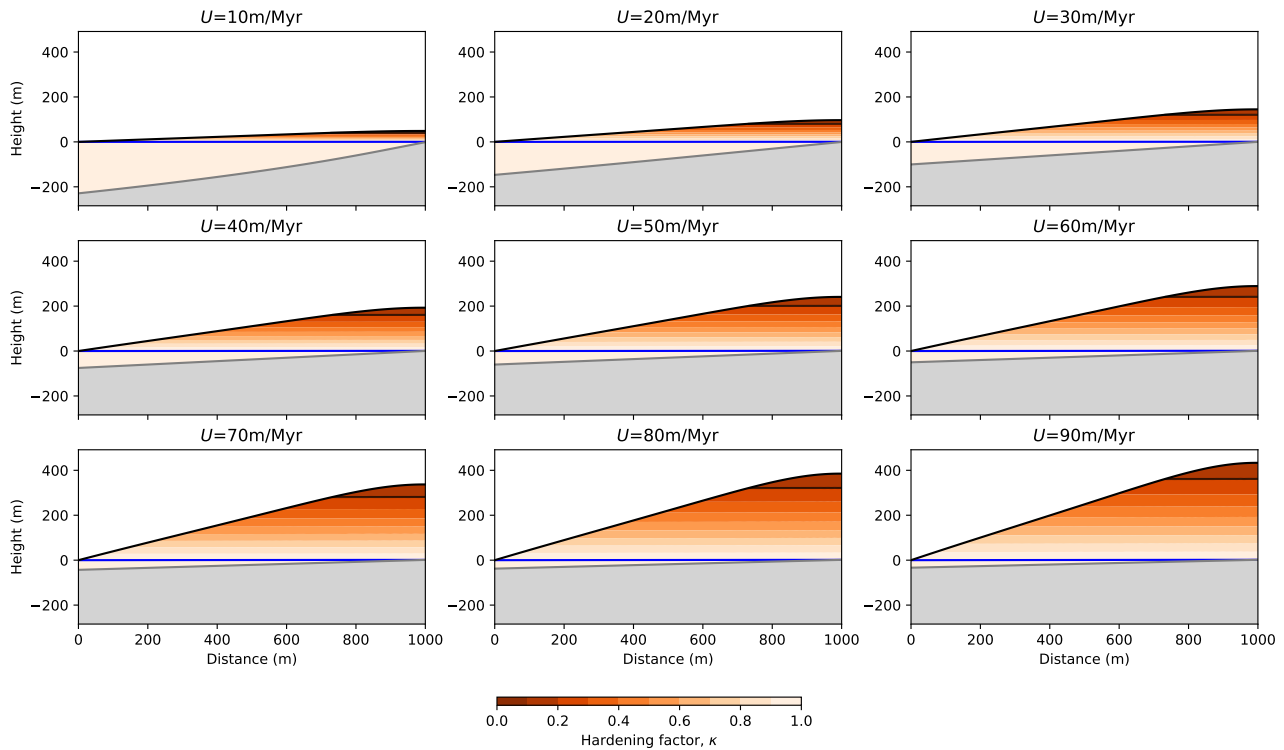


Figure S2. Model behavior with varying U , the uplift rate, in the percolation mode ($C = -1$). Each panel corresponds to the model solution after 20 Myr of evolution with a different value of U increasing from top left to bottom right.

S1.3 Varying U and K_D in percolation mode

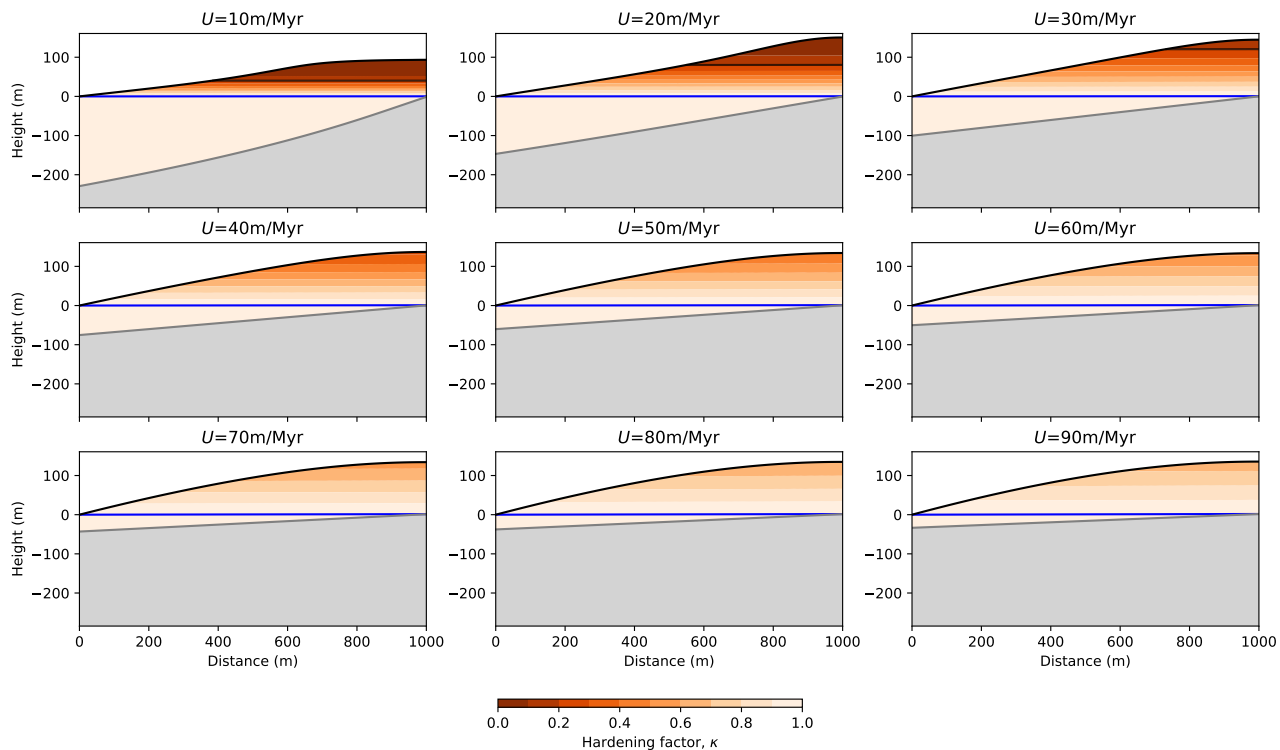


Figure S3. Model behavior with varying U , the uplift rate, and K_D , the surface transport coefficient in a constant ratio, in the percolation mode ($C = -1$). Each panel corresponds to the model solution after 20 Myr of evolution.

5 S1.4 Varying P in percolation mode

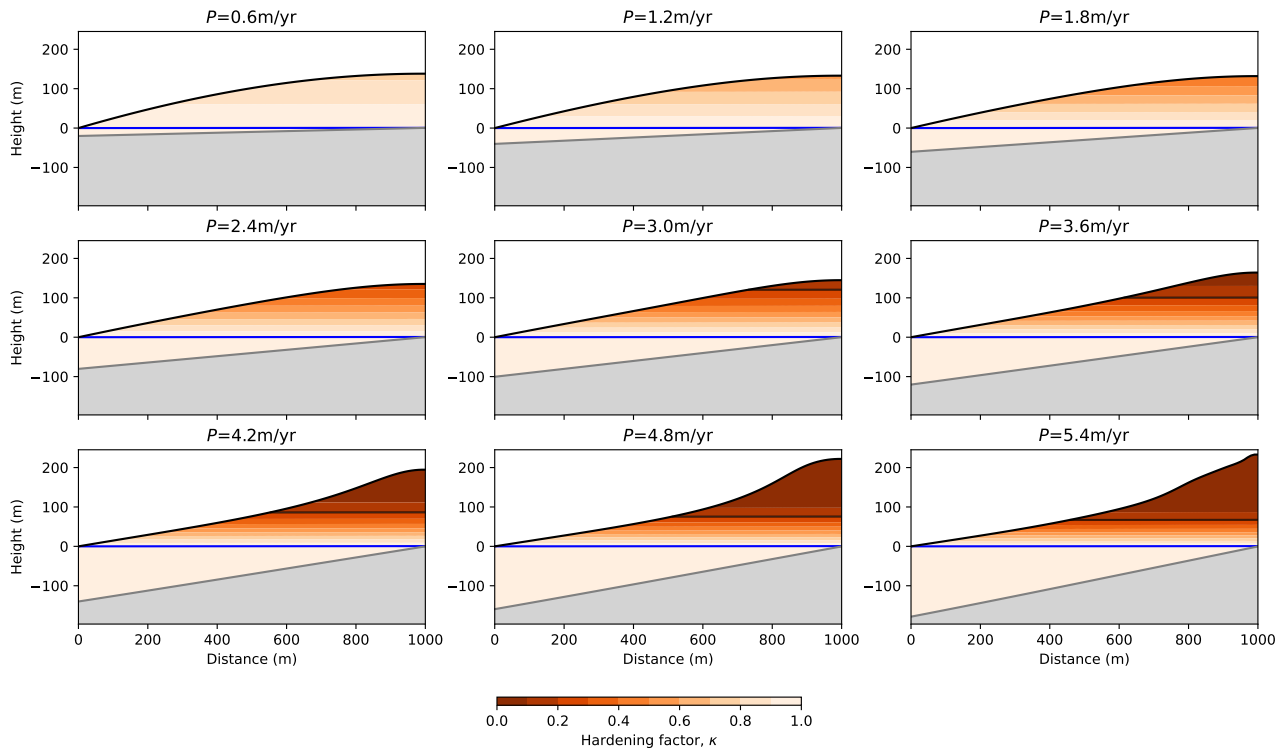


Figure S4. Model behavior with varying P , the precipitation or surface infiltration rate, in the percolation mode ($C = -1$). Each panel corresponds to the model solution after 20 Myr of evolution.

S1.5 Varying τ_m in percolation mode

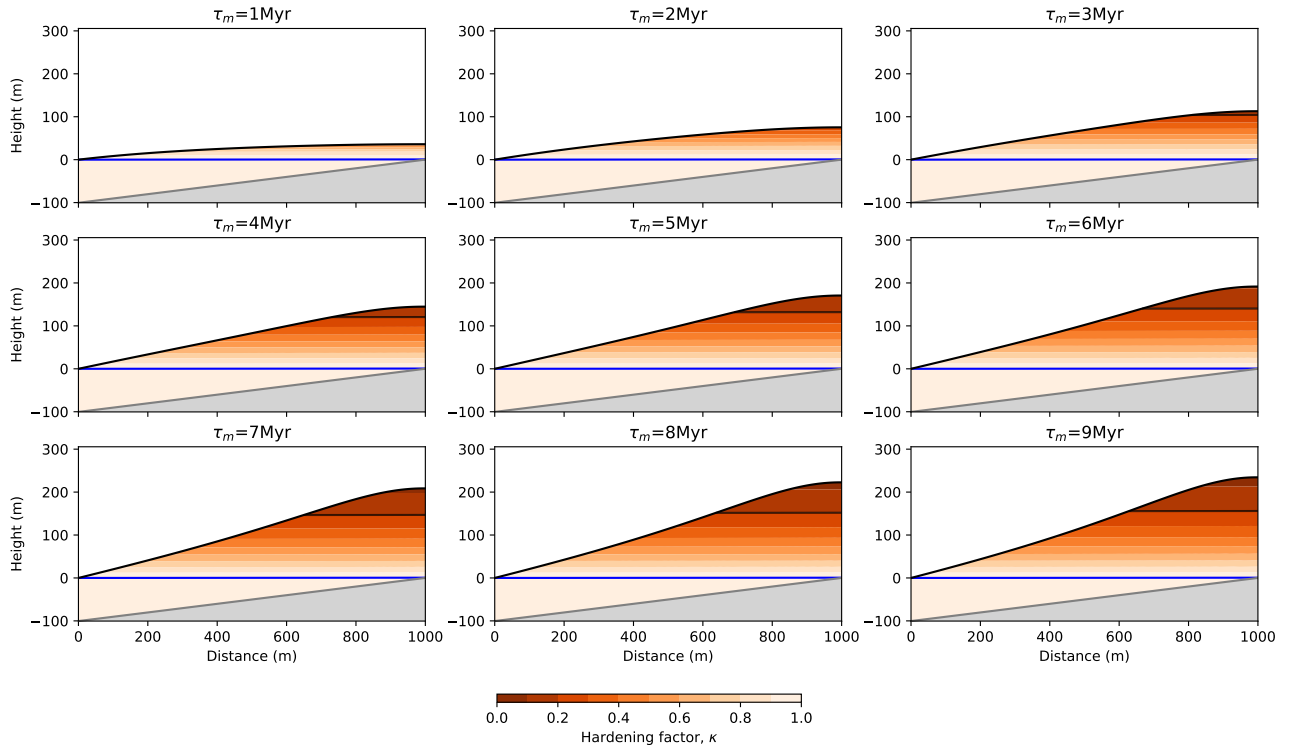


Figure S5. Model behavior with varying τ_m , the mass loss time scale, in the percolation mode ($C = -1$). Each panel corresponds to the model solution after 20 Myr of evolution.

S1.6 Varying τ in saturated mode

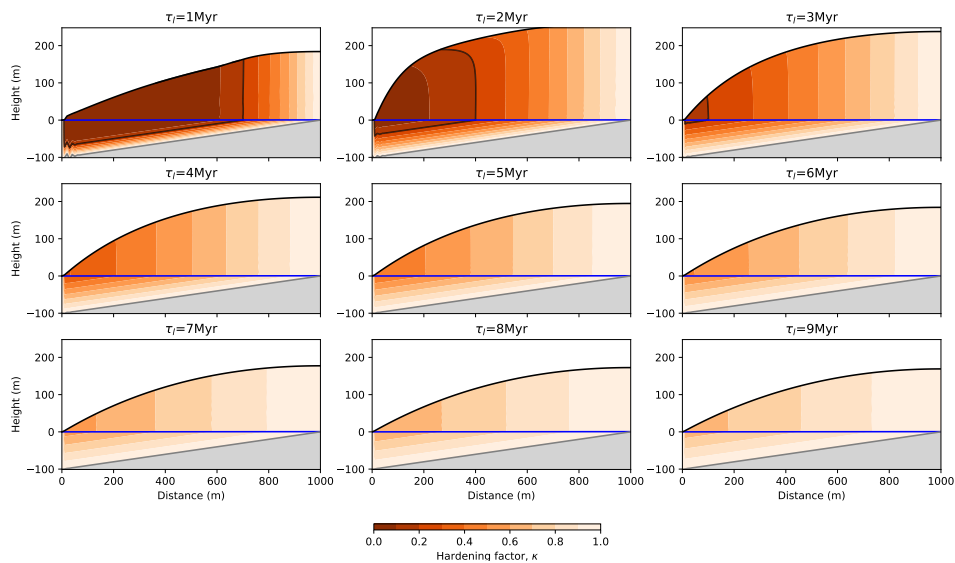


Figure S6. Model behavior with varying τ , the laterisation time scale, in the saturated mode ($C = 0$). Each panel corresponds to the model solution after 20 Myr of evolution with a different value of τ increasing from top left to bottom right.

S1.7 Varying U in saturated mode

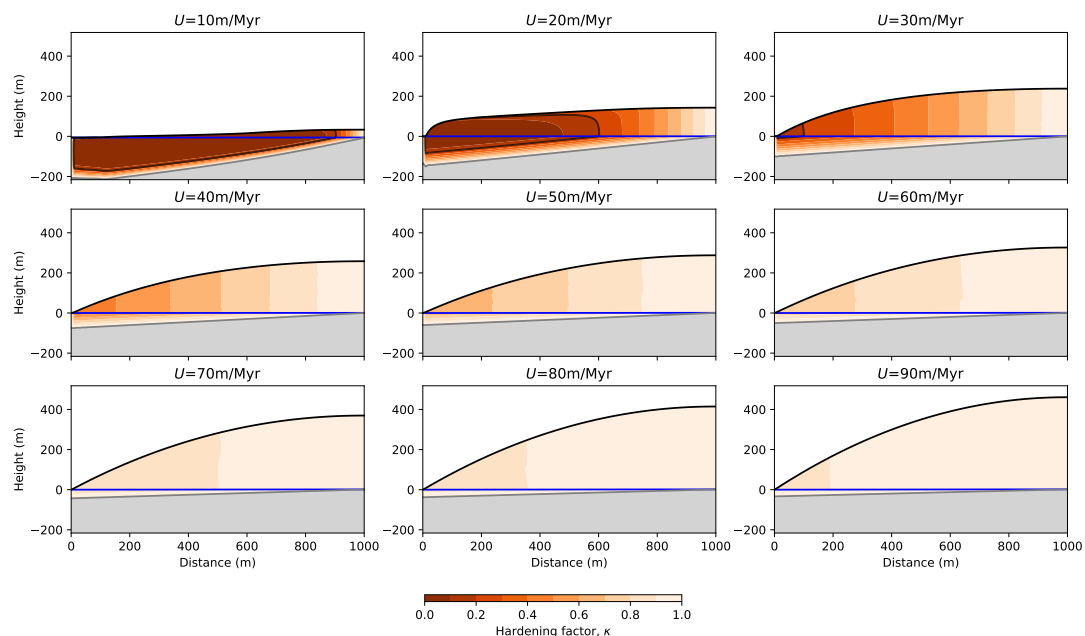


Figure S7. Model behavior with varying U , the uplift rate, in the saturated mode ($C = 0$). Each panel corresponds to the model solution after 20 Myr of evolution with a different value of U increasing from top left to bottom right.

S1.8 Varying U and K_D in saturated mode

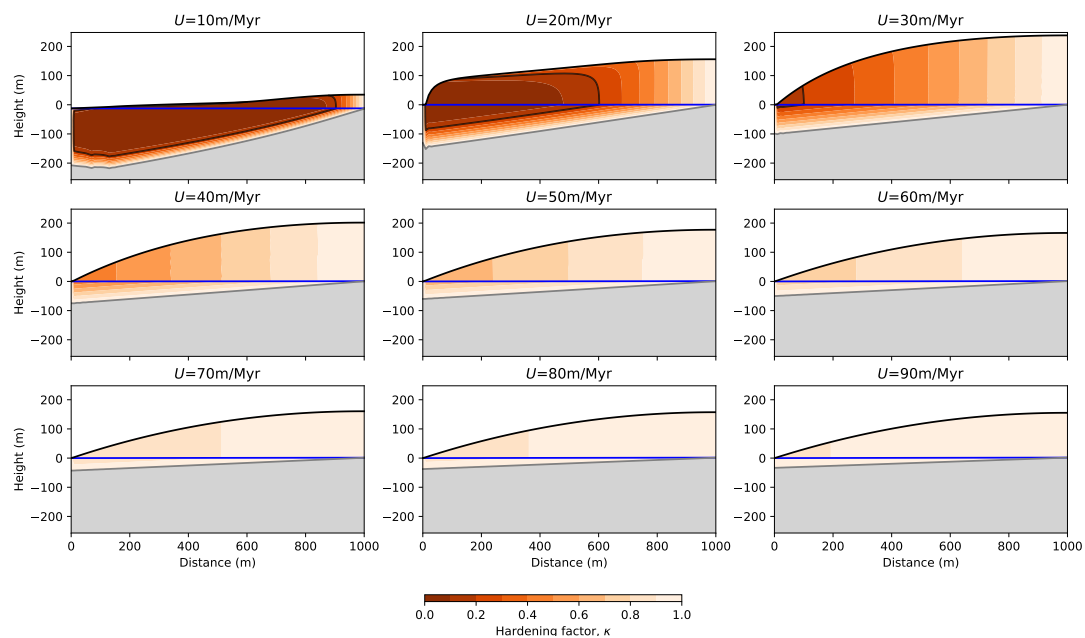


Figure S8. Model behavior with varying U , the uplift rate, and K_D , the surface transport coefficient in a constant ratio, in the saturated mode ($C = 0$). Each panel corresponds to the model solution after 20 Myr of evolution.

10 S1.9 Varying P in saturated mode

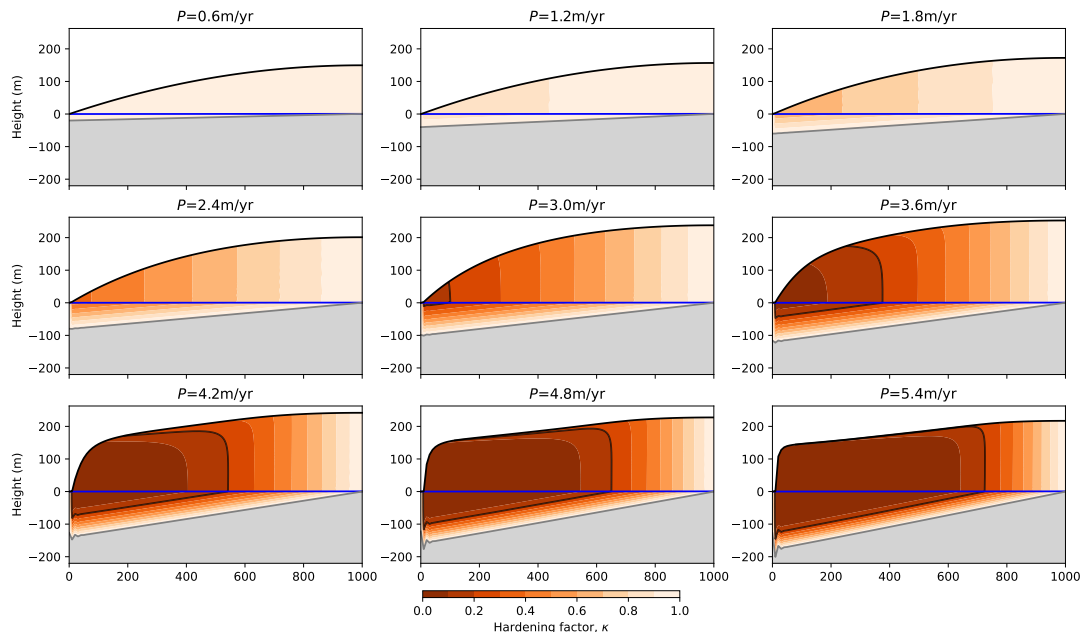


Figure S9. Model behavior with varying P , the precipitation or surface infiltration rate, in the saturated mode ($C = 0$). Each panel corresponds to the model solution after 20 Myr of evolution.

S1.10 Varying τ_m in saturated mode

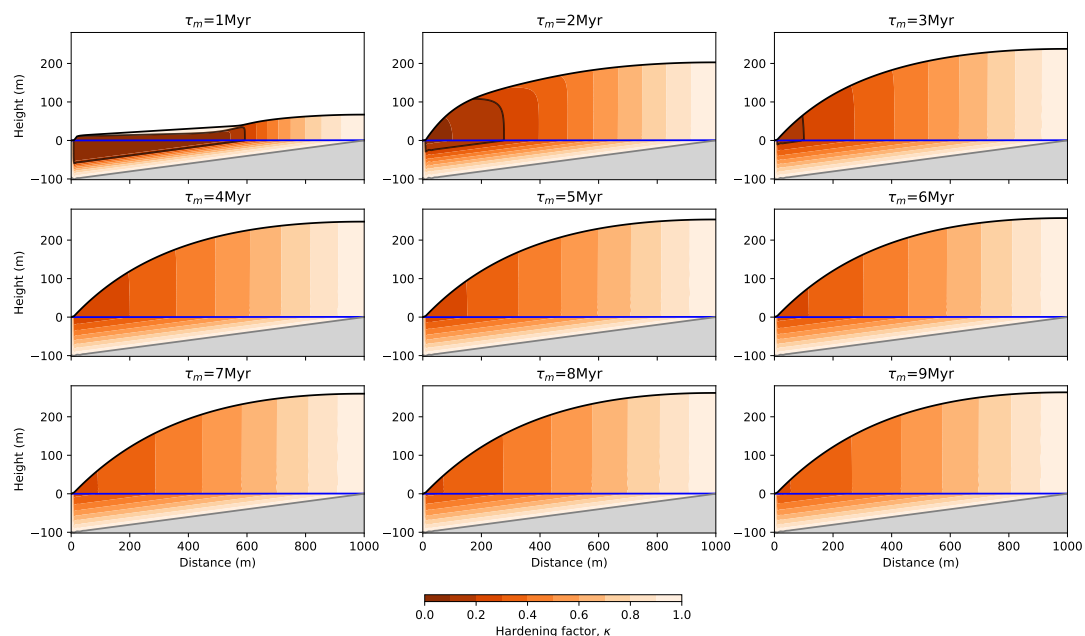


Figure S10. Model behavior with varying τ_m , the mass loss time scale, in the saturated mode ($C = 0$). Each panel corresponds to the model solution after 20 Myr of evolution.

S1.11 Varying τ in everywhere mode

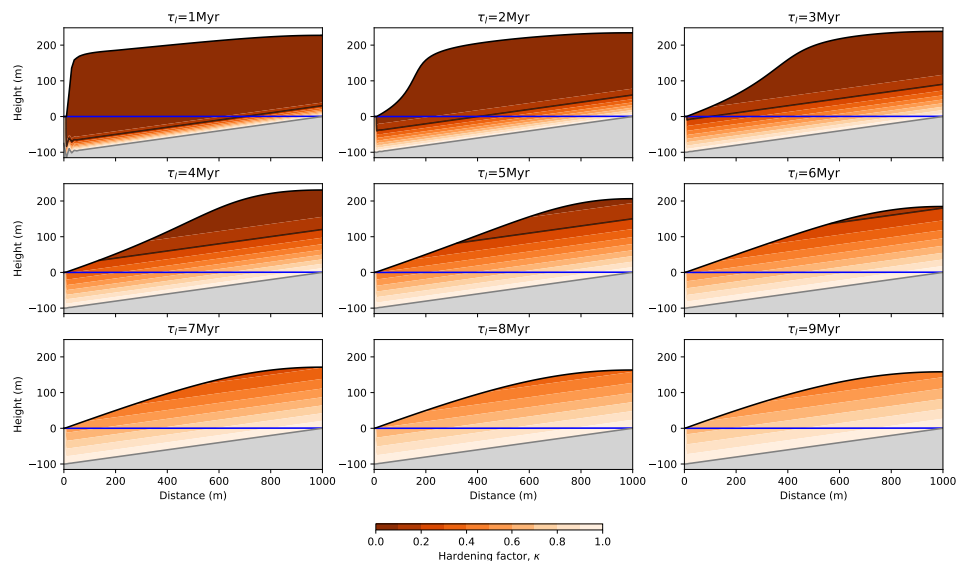


Figure S11. Model behavior with varying τ , the laterisation time scale, in the everywhere mode ($C = 1$). Each panel corresponds to the model solution after 20 Myr of evolution with a different value of τ increasing from top left to bottom right.

S1.12 Varying U in everywhere mode

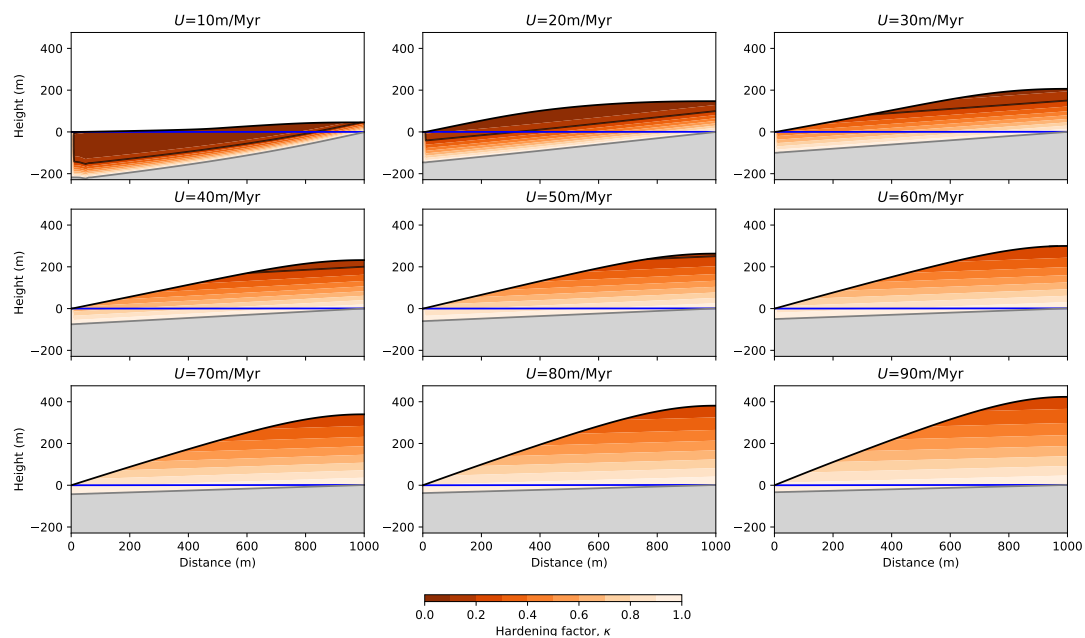


Figure S12. Model behavior with varying U , the uplift rate, in the everywhere mode ($C = 1$). Each panel corresponds to the model solution after 20 Myr of evolution with a different value of U increasing from top left to bottom right.

S1.13 Varying U and K_D in everywhere mode

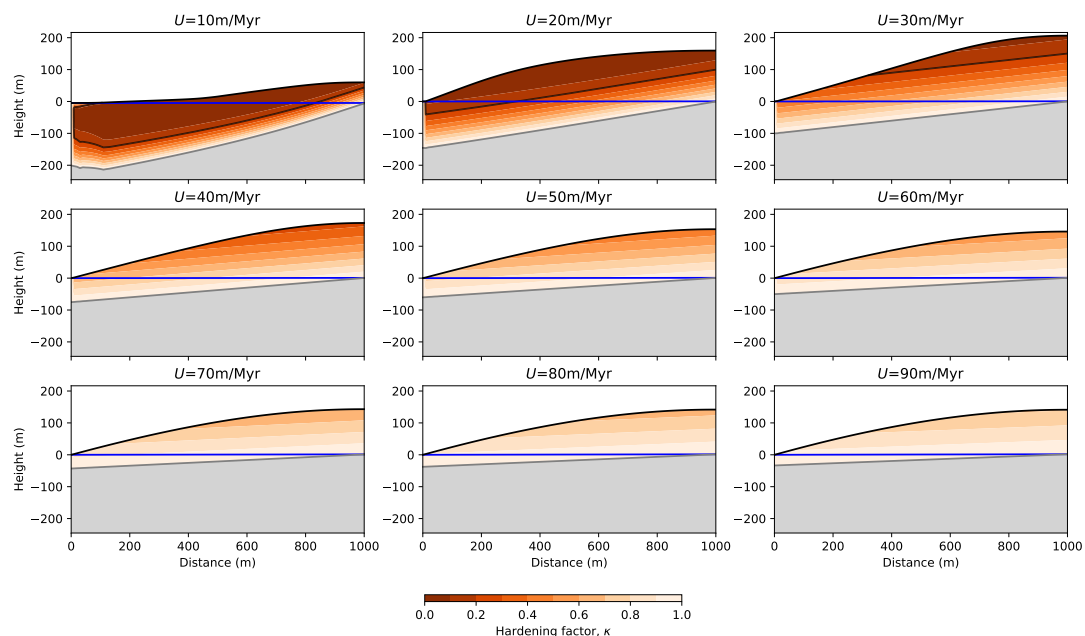


Figure S13. Model behavior with varying U , the uplift rate, and K_D , the surface transport coefficient in a constant ratio, in the everywhere mode ($C = -1$). Each panel corresponds to the model solution after 20 Myr of evolution.

15 S1.14 Varying P in everywhere mode

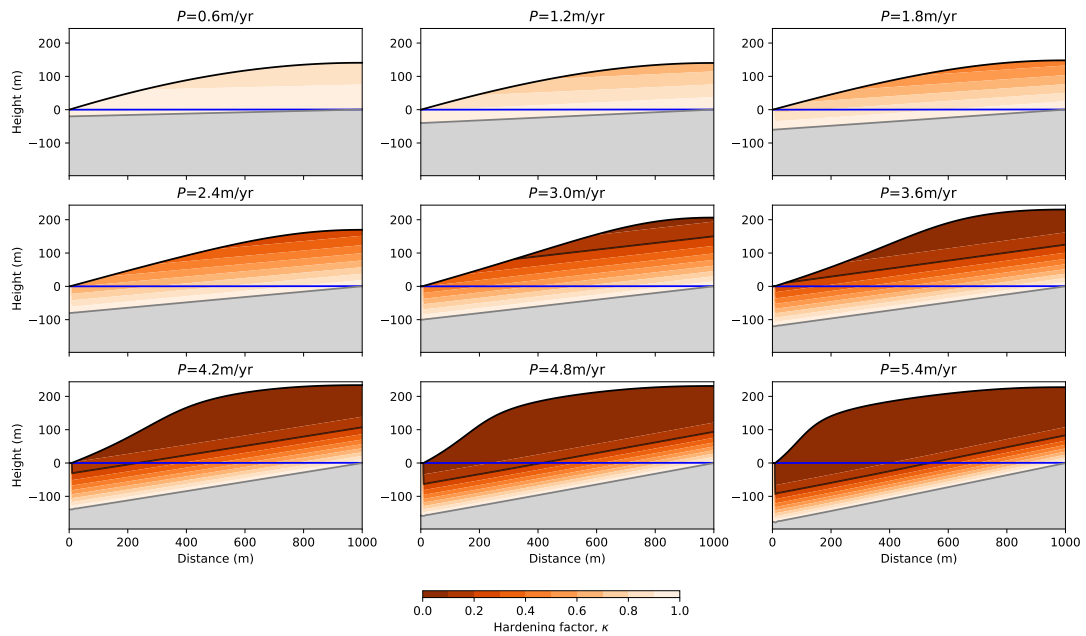


Figure S14. Model behavior with varying P , the precipitation or surface infiltration rate, in the everywhere mode ($C = 1$). Each panel corresponds to the model solution after 20 Myr of evolution.

S1.15 Varying τ_m in everywhere mode

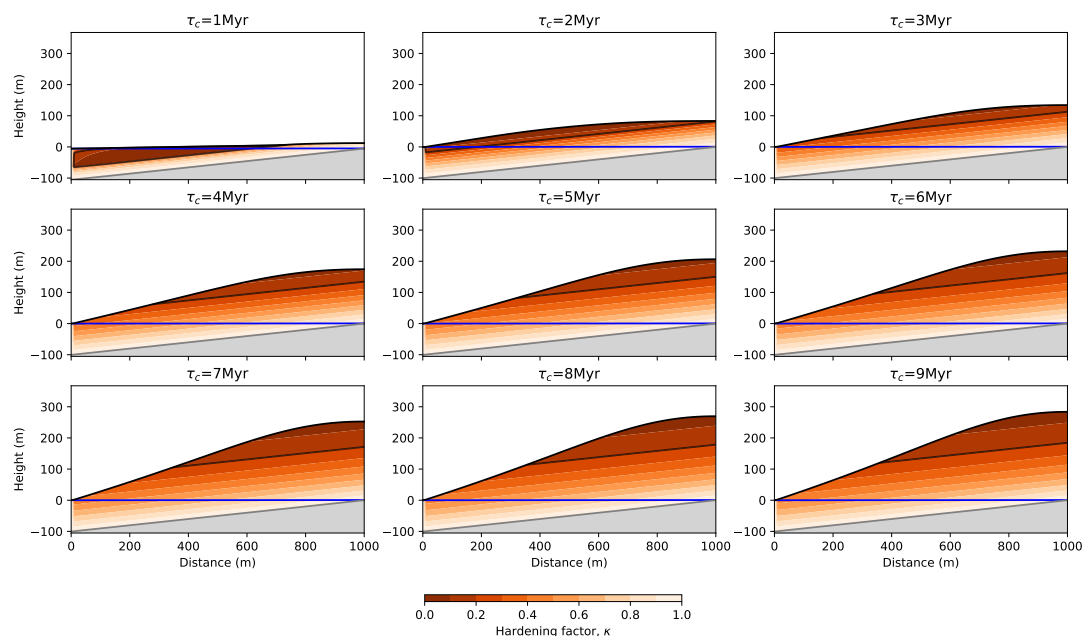


Figure S15. Model behavior with varying τ_m , the mass loss time scale, in the everywhere mode ($C = 1$). Each panel corresponds to the model solution after 20 Myr of evolution.

S1.16 Periodic variations in uplift rate in everywhere mode

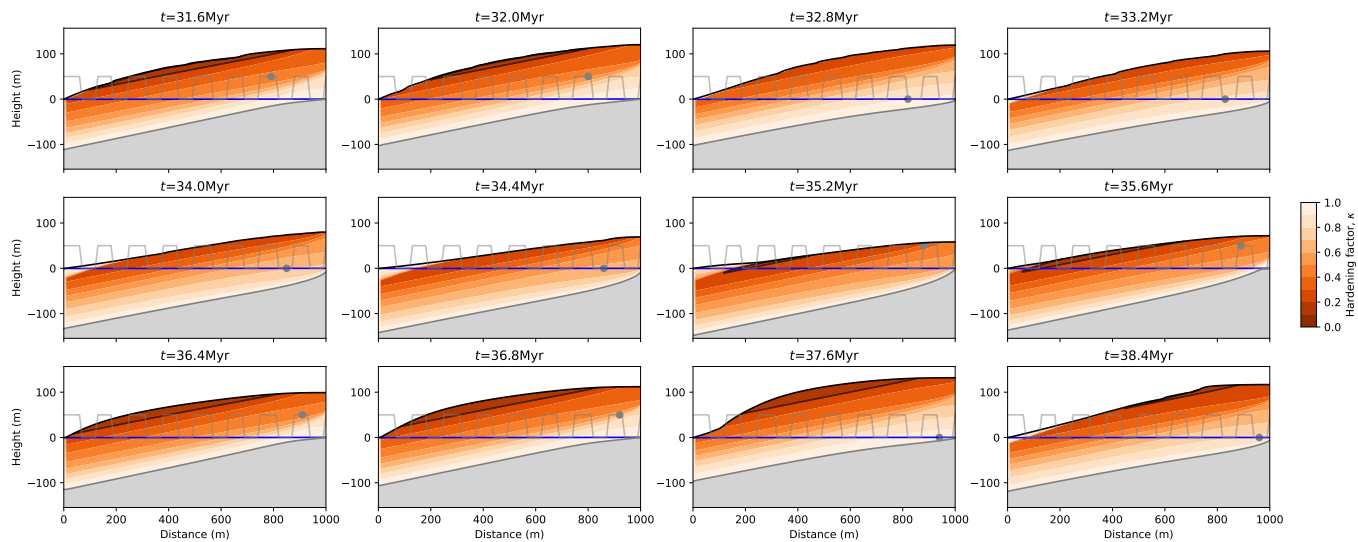


Figure S16. Varying the uplift rate by introducing periods of quiescence ($U = 0$) and active uplift ($U = 50 \text{ m Myr}^{-1}$) of equal duration as in Figure 11 but with $C = 1$, i.e., in everywhere mode.

S1.17 Periodic variations in precipitation rate in everywhere mode

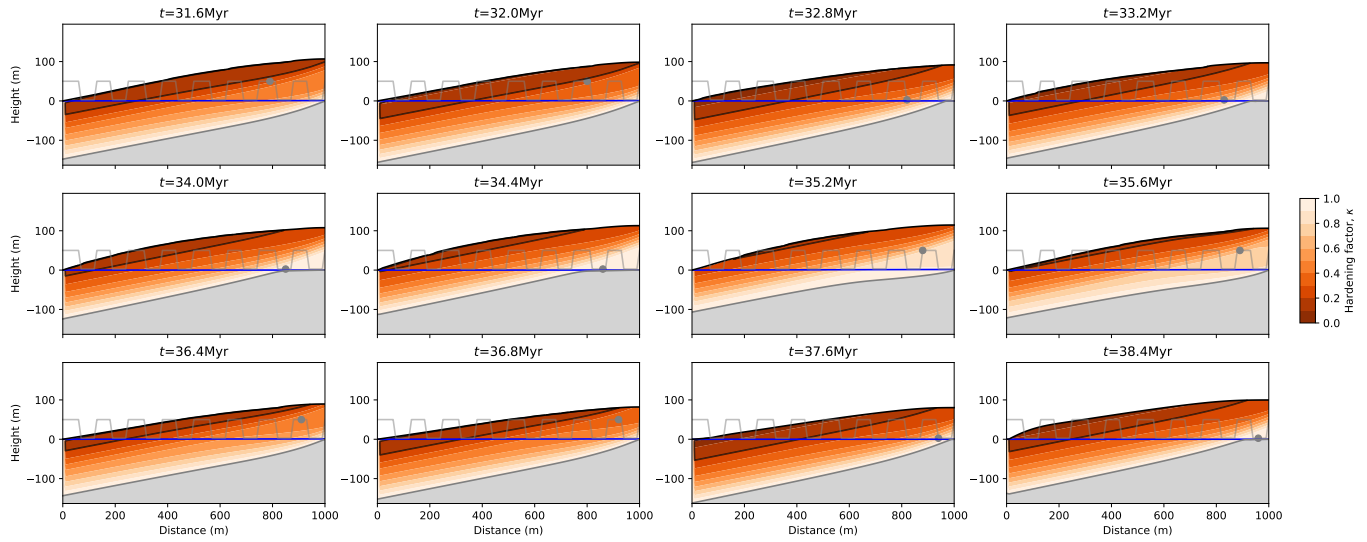


Figure S17. Varying the precipitation rate by introducing dry ($P = 0.5 \text{ m yr}^{-1}$) and wet ($P = 7.5 \text{ m yr}^{-1}$) periods of equal duration as in Figure 14 but with $C = 1$, i.e., in everywhere mode.

S1.18 Computed spectra

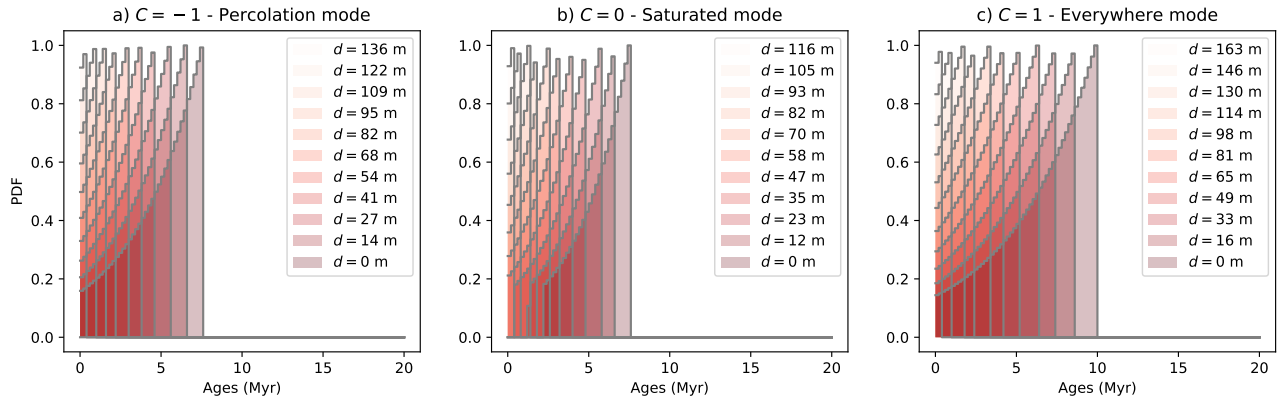


Figure S18. Computed age spectra along vertical profiles shown in Figure 16.

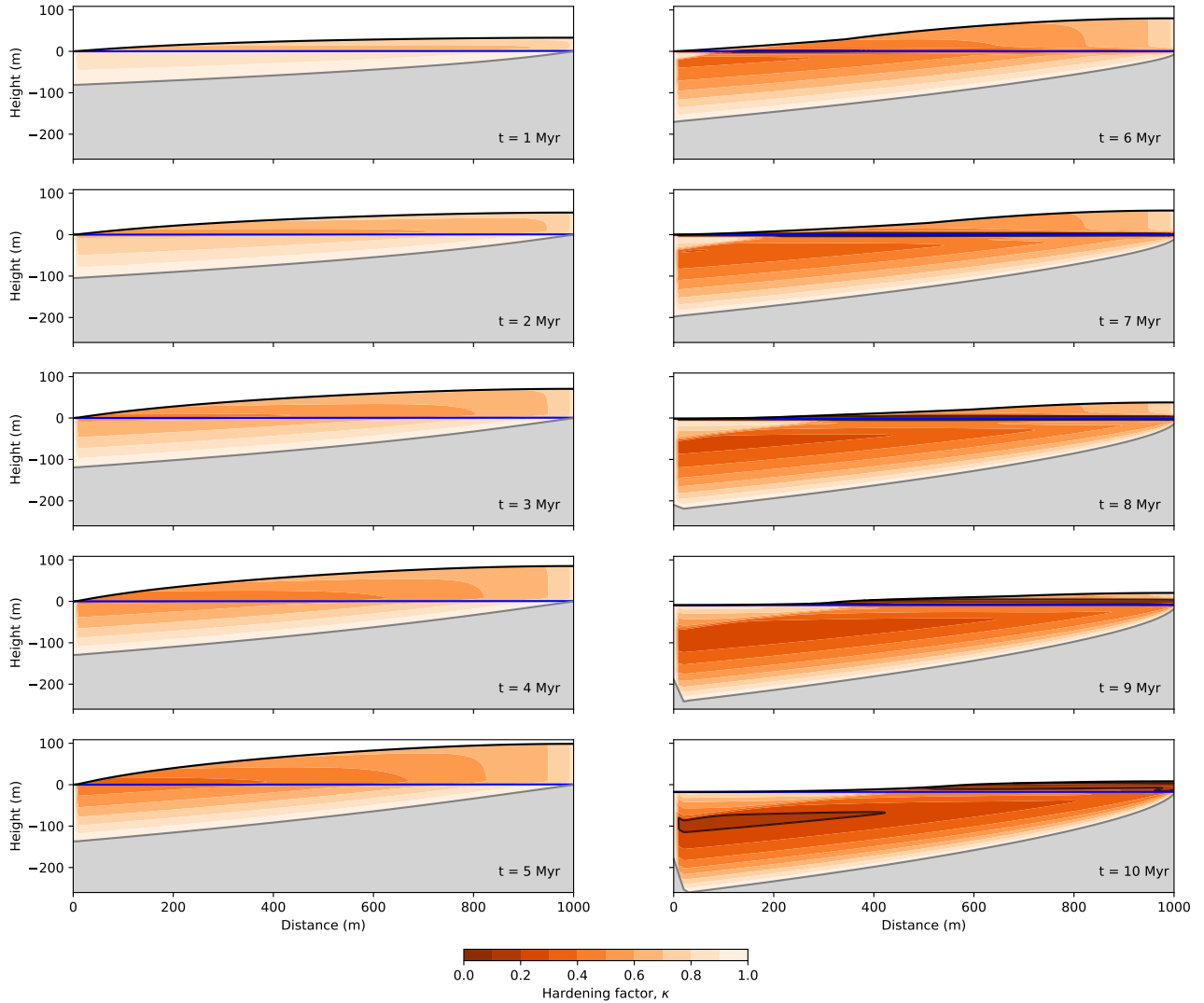


Figure S19. Evolution of a model experiment in which the LAT and WTF models have been combined. $U = 30 \text{ m Myr}^{-1}$ during the first half of the experiment and $U = 0 \text{ m Myr}^{-1}$ in the second half.